Taylor & Francis
Taylor & Francis Group

High Pressure Research
An International Journal

ISSN: 0895-7959 (Print) 1477-2299 (Online) Journal homepage: http://www.tandfonline.com/loi/ghpr20

RIXS in correlated electron systems under extreme conditions

V. Balédent & J.-P. Rueff

To cite this article: V. Balédent & J.-P. Rueff (2016): RIXS in correlated electron systems under extreme conditions, High Pressure Research, DOI: 10.1080/08957959.2016.1208819

To link to this article: http://dx.doi.org/10.1080/08957959.2016.1208819

Published online: 27 Jul 2016.

HIGH PRESSURE RESEARCH, 2016
http://dx.doi.org/10.1080/08957959.2016.1208819

Taylor & Francis
Taylor & Francis Group

RIXS in correlated electron systems under extreme conditions

V. Balédent[a] and J.-P. Rueff[b,c]

[a]Laboratoire de Physique des Solides, Université Paris-Sud, Orsay, France; [b]Synchrotron SOLEIL, L'Orme des Merisiers, Gif sur Yvette, France; [c]Laboratoire de Chimie Physique-Matière et Rayonnement, Sorbonne Universités, UPMC Université Paris 06, CNRS UMR 7614, Paris, France

ABSTRACT
We report here on the application of Resonant Inelastic X-ray Scattering (RIXS) in correlated electrons systems under pressure. Thanks to its bulk sensitivity and superior resolving power, RIXS appears as a powerful spectroscopic technique to unravel the local electronic and magnetic properties of materials at extreme conditions. The method is illustrated in vanadium-oxides- and Fe-based superconductors at high pressure.

ARTICLE HISTORY
Received 1 May 2016
Accepted 20 June 2016

KEYWORDS
RIXS; correlated electron systems; extreme conditions

1. Introduction

1.1. Correlated electrons systems under pressure

Pressure is an effective means to alter the electronic density in solids. In correlated materials where electrons are strongly coupled to the other degrees of freedom (lattice, orbital and spin), this has dramatic consequences. Applying pressure may force closing the correlation gap through band-widening effect and leads to metal–insulator transition (MIT). Among the correlated oxides, this is best exemplified by the case of V_2O_3 (which undergoes an iso-structural MIT under pressure) or VO_2, which is discussed in this manuscript. In heavy fermion materials, pressure can trigger a delocalization of the f-electrons, or destabilize the magnetic order. In these materials, new exotic phases may emerge under pressure such as nonconventional superconductivity or the onset of a quantum critical point. Superconductivity was also disclosed in several 3d materials such as Fe-based superconductors, where pressure can be seen as an external way to dope the conduction band through the renormalization of the band structure in a compressed lattice. Finally, by shortening the atomic distance, pressure acts directly onto the strength of the crystal field. In 3d correlated oxides for instance, this may modify the spin state [1] and alter the structural stability.

1.2. RIXS spectroscopy

Resonant inelastic X-ray scattering (RIXS) is a powerful technique for the investigation of the electronic properties of materials. With the advent of new high-resolution spectrometers, RIXS has been increasingly used in the soft-X-rays for revealing the low

CONTACT J.-P. Rueff jean-pascal.rueff@synchrotron-soleil.fr

energy excitations of correlated materials. The intense resonance at the $L_{2,3}$ edges of 3d metals and the specific nature of the RIXS cross section makes it possible to study spin, charge or orbital excitations and their dispersion.[2] Yet, soft-X-ray RIXS is blind to samples contained in strongly absorbing environments such as pressure cells because of the poor penetration depth of low-energy photons. This is no longer true for hard-X-ray (5 keV) RIXS, opening up new perspectives for the study of materials at extreme conditions.[3] In fact, part of the information contained in soft-X-ray XAS can be retrieved from hard-X-ray RIXS. For instance, the $L_{2,3}$ edges XAS can be compared to the 1s2p-RIXS process. The former is governed by $2p \rightarrow 3d$ transitions, while the later implies the absorption $1s \rightarrow (3d)4p$ (considering dipolar transitions to 4p and quadrupolar to 3d states) and $2p \rightarrow 1s$ decay. In both cases, the final state consists of a 2p core-hole and additional electron in the 3d band so that the $L_{2,3}$ XAS states should be visible in the 1s2p-RIXS plane [4] (providing interference effects are neglected [5]). This analogous behavior makes it possible to approach soft-X-ray magnetic circular dichroism with RIXS hard-X-ray using circularly polarized photons.[6] When departing from the resonant conditions, the IXS process yields the energy loss spectra of a materials. Using hard-X-ray photons, it is then possible to measure the absorption K-edges of light elements that normally falls in the soft-X-rays' range. The method (usually referred to as X-ray Raman Scattering) has strong implications for high pressure research, as reported elsewhere in this issue.[7,8]

Thus, as discussed in the following, RIXS and its associated techniques (emission spectroscopy and high-resolution X-ray absorption) provides a means to investigate the whole variety of pressure-induced phenomena. We illustrate in this study the use of RIXS in different correlated systems under pressure, including a prototypical Mott insulator VO_2, and the Fe-superconductors $BaFe_2As_2$. A large part of the experimental data was acquired on the recently commissioning hard-X-ray spectroscopy GALAXIES beamline at SOLEIL synchrotron.[9]

2. Methodology

2.1. RIXS measurements

RIXS is a photon-in–photon-out spectroscopy that can be formally described by the Kramers–Heisenberg second-order formula. RIXS involves the excitations of core electrons under interaction with the incident X-rays photons (of energy E_1) followed by the radiative decay of the excited atom with emission of a secondary photon (with energy E_2) as shown in Figure 1(a). In the RIXS process, the incident photon energy is normally chosen near an absorption edge so that emission cross section is modulated by the absorption process. In the simple case, the incident photon energy is chosen sufficiently far above the absorption edge so that the RIXS process limits itself to fluorescence. For clarity reasons, one usually distinguishes core-level emission (dashed blue line in Figure 1(a)) from the emission originating from valence band electrons (solid blue line in Figure 1(a)).

When E_1 approaches a resonance, the absorption and emission processes can no longer be treated independently. The full process involves a spectral map that expresses the variation of the RIXS intensity as a function of the incident (E_1) and transfer energy ($E_1 - E_2$) as illustrated in Figure 1b(1) for a simplistic modeling of the RIXS cross section. Specific cuts or projection can be extracted from the spectral map: The projected intensity along E_1 provides the absorption spectrum as measured by total fluorescence yield (TFY) mode

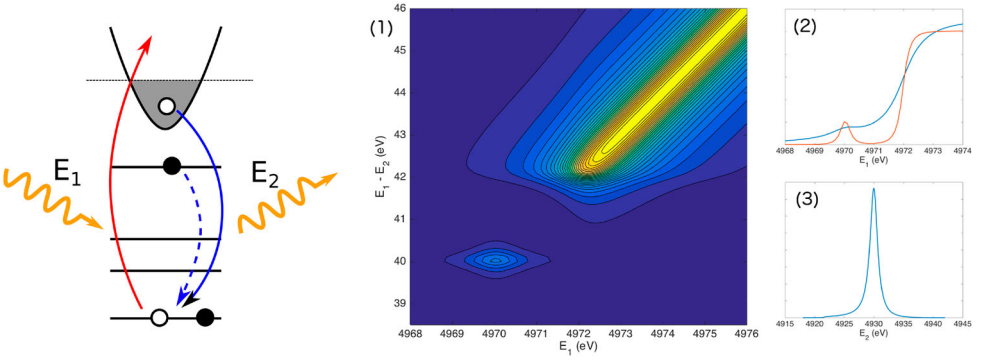

(a) RIXS one electron picture (b) RIXS map

Figure 1. (Left) RIXS process in a one-electron picture. (Right): RIXS simulated spectral intensity map (1) as a function of the incident (E_1) and transfer energy ($E_1 - E_2$) ; blue lines in (2) and (3) are the projected intensity vs. E_1 and E_2 representative of the absorption (XAS) and emission (XES) spectra. The red line in panel (2) is a cut at 45° in (1) and depicts the PFY-XAS high-resolution process. (a) RIXS one-electron picture and (b) RIXS map.

(blue line in Figure 1b(2)) while the projection along E_2 yields the fluorescence line (*cf.* Figure 1b(3)). A sharper version of the TFY absorption spectrum can be obtained by fixing the emitted energy (E_2) while sweeping the incident energy around the edge. In the spectral map of Figure 1, this corresponds to a cut along the diagonal. Compared to the TFY-XAS, the resulting partial fluorescence yield (PFY) spectrum (red line in Figure 1b(2)) exhibits a higher intrinsic resolution beyond standard XAS (red line in Figure 1b(2)). The difference comes from the shallower core-hole involved in the RIXS (PFY-XAS) finale state with respect to standard XAS.

2.2. Spectrometer and geometry

The RIXS measurements rely on the energy analysis of the scattered photons. Most RIXS spectrometers operating in the hard-X-ray region are based on the focusing, nondispersive Rowland circle geometry using spherically bent analyzers as illustrated in Figure 2(a). The sample, analyzer and detector are located on a virtual circle whose diameter matches the analyzer bending radius. The RIXS energy is scanned by changing the analyzer Bragg angle while moving the detector in order to maintain the Rowland focusing conditions. In the example of Figure 2(a), the Rowland circle rotates around the sample during the energy scan. In this configuration, the analyzer moves along a straight line which helps for mechanical implementation but other ways of scanning could be envisaged. At the GALAXIES beamline, the RIXS spectra are acquired in a continuous scanning mode that avoids motion dead times using nonlinear trajectories of the detector as depicted in Figure 2(a).

2.3. High pressure X-ray spectroscopy

To apply pressure, diamond anvil cells (DAC) stand out as a powerful, yet compact, apparatus. In the energy range (4–10 keV) we are interested in however, diamonds are still

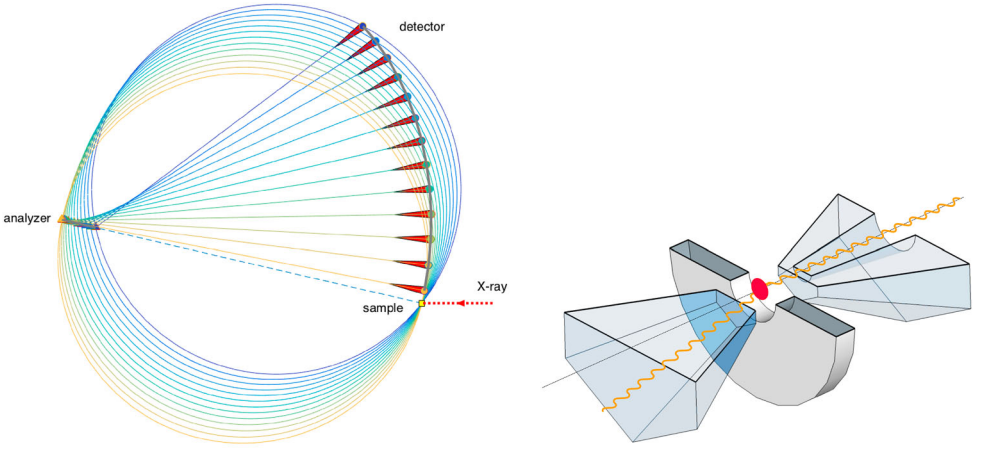

(a) RIXS geometry (b) Example of high pressure geometry

Figure 2. (a) RIXS circle geometry: the analyzer and detector trajectories are depicted for a scan of the Bragg angle of $77 \pm 12^{\circ}$ by step of 2°. Each color corresponds to one energy. (b) Schematic cut view of a diamond anvil cell for transmission geometry equipped with a partially perforated diamond on one side and a full diamond on the other side.

highly absorbing. DAC transmission can be improved in two ways: (1) using Be gasket with the photons emitted in the equatorial plane of the pressure cell (*cf.e.g.* Ref. [10] in this issue); (2) using thin diamonds as preferred in this work – *cf*. Figure 2(b). In the latter case, a single or a pair of partially perforated diamonds with a backwall of typical thickness of 200 μm are used. This allows a high transmission of more 50% from 6 keV onwards, and more than 10% at 4 keV while offering a large opening angle of 30° or more that suits well the RIXS geometry. Partially perforated diamonds being opaque to visible light, they cannot be used for ruby luminescence spectroscopy. Instead, a thin diamond plate (of ≈200 μm thickness) or slightly thicker miniature anvil (500 μm) can be mounted onto a fully perforated anvil. The thin plate offers high transmission for both X-ray and visible light but is reportedly more fragile that the miniature anvil.

The typical sample thickness in the DAC is about 20 μm. This requires thinning down the sample by either polishing or cleaving methods. Alternatively, powder samples can be used when the thinning process is difficult or when crystals are not available.

3. RIXS in correlated electron systems under pressure

We now turn to some specific and recent applications of RIXS in correlated electron systems under pressure with a focus on vanadium-oxides- and Fe-based superconductors.

3.1. Metal–insulator transition: case of V oxides

The MIT is a crucial manifestation of the correlated nature of Mott insulators. From band theory, these materials are expected to be metallic but instead show insulator properties.[11] As formalized by Mott,[12,13] this intriguing state is due to the strong on site

Coulomb repulsion U. In the strong limit, this may lead to an insulating state usually concomitant to antiferromagnetic ordering. Under pressure, U competes with the d-bandwidth (W), eventually leading to the closure of the correlation gap ($U<W$). The MIT can be more accurately grasped within the Dynamical Mean Field Theory.[14] RIXS was shown to be an effective means to investigate MIT under pressure in correlated materials. In the following, this is illustrated in two vanadium oxides (V_2O_3 and VO_2) considered as prototypical Mott insulators.

V_2O_3 is a paramagnetic insulator at ambient conditions and can be driven through an MIT by pressure, doping or temperature as illustrated in Figure 3(a). The isostructural, correlation-driven nature of the MIT has made V_2O_3 as one of the most studied correlated materials.

Early soft-X-ray XAS has been key to reveal in V_2O_3 the role of the spin and orbital dependence of the Coulomb energy [16] for the T dependent transition, ruling out the simplest one-band Hubbard model. More recently, high-energy RIXS was used to provide a complete survey of the phase diagram, especially dealing with the P-induced MIT. As pressure can be continuously varied, RIXS can be performed while approaching the MIT. In this work, PFY-XAS was carried out at the V K-edge, as shown in Figure 4(a) along different pathways (P, T and doping (x)) in the phase diagram.[17,18] Here, RIXS serves to highlight the pre-edge features that are sensitive to the V-d states. The superior resolution of RIXS helps us to overcome the limits of sensitivity of standard XAS. The results show that different metallic states can be reached depending on the control parameters. This is likely related to the coexistence of the different phases as demonstrated independently by spectromicroscopy.[19]

Unlike V_2O_3, the T-induced MIT in VO_2 is accompanied by a structural distortion with a doubling of the crystal unit cell from a rutile R to a monoclinic M_1 phase [20] while Cr doping produces two additional insulating phases (M_2, T) [21] as shown in Figure 3(b). To disentangle the respective role of structural and electronic degrees of freedom has been quite a challenge. Under high pressure Raman, Arcangeletti et al. observed hints

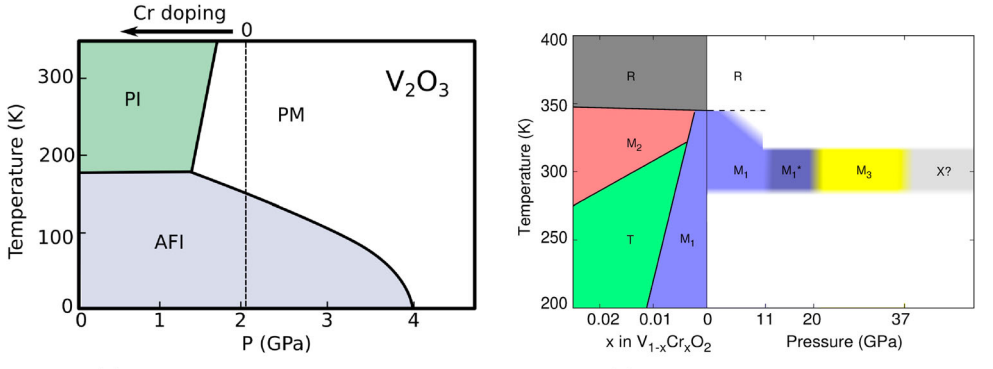

(a) Phase diagram of V_2O_3 (b) Phase diagram of VO_2

Figure 3. (a) Simplified phase diagram of V_2O_3 as a function of pressure (P), doping (x) and temperature (T); PI, PM and AFI stand for the paramagnetic insulating, paramagnetic metallic and antiferromagnetic insulating states (adapted from Ref. [15]). (b) Schematic phase diagram of VO_2 as a function of doping, pressure and temperature (see text for details).

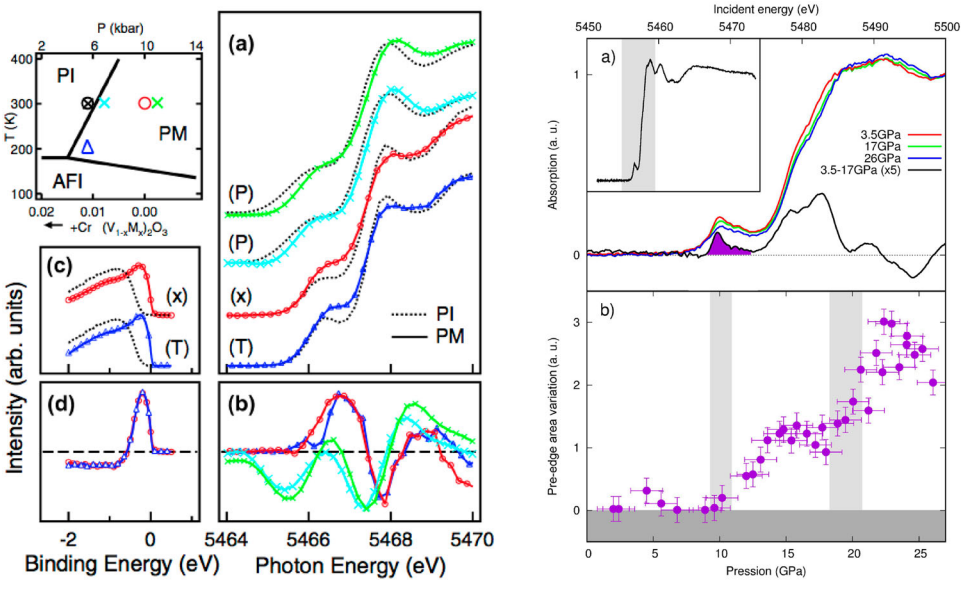

(a) RIXS results in V_2O_3 (b) RIXS results in VO_2

Figure 4. (a) RIXS-derived V K pre-edge spectra for powder sample of Cr-doped V_2O_3 as a function of *P* (crosses), *T* (triangles) and *x* (circles) – *cf.* points loci in the top left phase diagram. (b) Differences between insulating and metallic spectra for the different parameters through the MIT (from Ref. [17]). (b) RIXS-derived near-edge absorption spectra for VO_2 at room temperature at low pressure (M_1 phase, 3.5 GPa), intermediate pressure (M_1* phase, 17 GPa) and high pressure (M_3 phase, 26 GPa)(a). The full spectrum is shown in the inset. The black curve represents the difference between 3.5 and 17 GPa (multiplied by a factor of 5 for more visibility); (b) pressure dependence of the integrated intensity of the difference with respect to the low pressure, in the energy range shown by the purple area in panel (a).

of metallization above 11 GPa at room temperature,[22] simultaneously with a change in bulk modulus without structural transition as revealed by X-ray diffraction.[23] This change in electronic properties without space group change suggests a modification of the properties driven by electronic degrees of freedom.

Similar to what was done for V_2O_3, RIXS at the V K-edge was applied in VO_2 under pressure (Figure 4(b)). The results show that the electronic structure is strongly affected between 3.5 GPa (insulating state) and 17 GPa, where the metallization has already occurred. The transition seems to occur around 11 GPa, where the RIXS PFY-XAS spectra lineshape start to deviate from the insulating state in agreement with [22]. The change of the electronic structure is yet to be understood, but is likely to be responsible for the progressive metallization. The high pressure electronic state seems to remain stable from 15 GPa up to 20 GPa. Above 20 GPa, a novel phase (denoted M_3 in Figure 3(b)) seemingly occurs that we recently confirmed by Raman spectroscopy,[24] likely followed by yet another phase (*X*) as recently reported by X-ray diffraction.[25] The spectral changes observed in the pre-edge region can be due to the variation of the orbital occupancy or local modification around the vanadium sites. Below 11 GPa no structural transition has been reported, implying that the observed behavior is primarily related to a modification of the 3d orbital occupancy. Above 20 GPa, however our Raman spectroscopy data [24]

suggest a structural phase transition. This is likely to affect the pre-edge structure and add to the change of the spectral weight in this region.

3.2. Unconventional superconductivity: Fe-based superconductors

The layered iron-based pnictides (FeSC) have emerged recently as a new class of high-temperature superconductors with intriguing properties. The FeSC consists of FeAs layers separated by pnictogen, chalcogen or rare-earth oxide blocking layers. Soon after the first report of superconductivity in LaFeAsO ($T_c = 26$ K), numerous other compounds with higher critical temperature were discovered such as SmFeAsO ($T_c = 55$ K) or $BaFe_2As_2$, offering a complete new set of materials for the study of unconventional superconducting state. Most of Fe pnictides share the same generic phase diagram illustrated in Figure 5. The parent compound generally undergoes a magnetic transition at low temperature almost concomitant to a tetragonal to orthorhombic structural transition. Upon doping or applying pressure, both structural and magnetic transitions progressively vanish while superconductivity settles with a dome-shaped critical temperature as a function of doping or pressure.

RIXS can help investigating the role of doping and pressure on the electronic structure of the Fe–As active planar layer. RIXS was applied in at the Fe K-edge and As K-edge respectively to determine the respective modifications of the Fe and As electronic properties thanks to superior resolving power of RIXS with respect to standard XAS. The results are summarized in Figure 6. The Fe spectra show a well-defined pre-edge (around 7110 eV) related to the 3d-states followed by a intense white line reminiscent of the p-states. Whereas the Fe K-edge shows a surprising insensitivity to both control parameters, the As K-edge exhibits a strong pressure and doping dependence.[27,28] These results are in apparent contradiction with photoemission measurements that indicate a filling of the Fe-3d bands upon doping. On the other hand, they seemingly confirm the non-local doping model derived from DFT calculations.[29]

Another interesting feature of RIXS in 3d ions relies in its capacity to probe the element-dependent spin state and conduction band with bulk sensitivity. The spin state can be derived from measurements of the Kβ (or Kα) emission line as illustrated in Figure 7 for the 122 family. The change of the Kβ lineshape is indicative of a redistribution of the

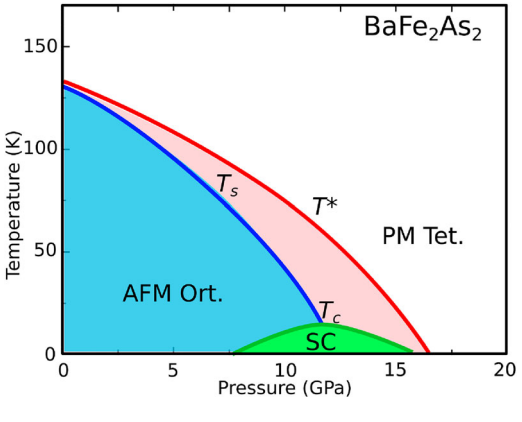

Figure 5. Schematic phase diagram of the 122 Fe-based superconductor (adapted from. Ref. [26]). T_c, T_s and T^* represent the critical, structural transition and magnetic order temperatures.

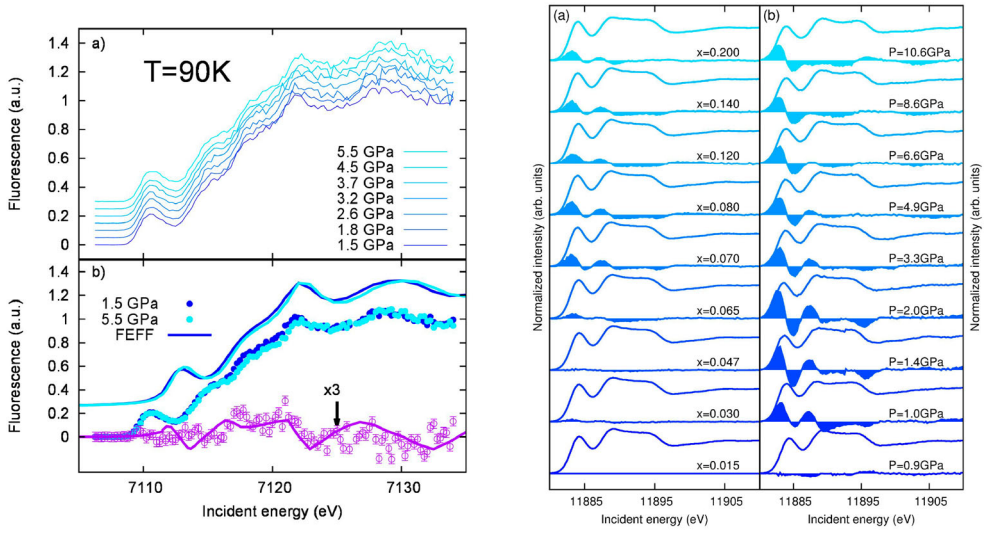

(a) Fe K-edge PFY-XAS (from Ref. [27]) (b) As K-edge PFY-XAS (from Ref. [28])

Figure 6. RIXS in the 122 Fe-based superconductor. (a) Fe K-edge PFY-XAS (from Ref. [27]) and (b) As K-edge PFY-XAS (from Ref. [28]).

local spin state population on the 3d atom. The spin information can be obtained via phenomenological approach as explained in Ref. [10] in the same issue for the 11 family or more generally by comparing with multiplet calculations.[30] We have recently used the sensitivity of the valence band (valence-to-core) emission (VBE) to follow more precisely the 3d-projected conduction states under pressure in selected materials of the 112

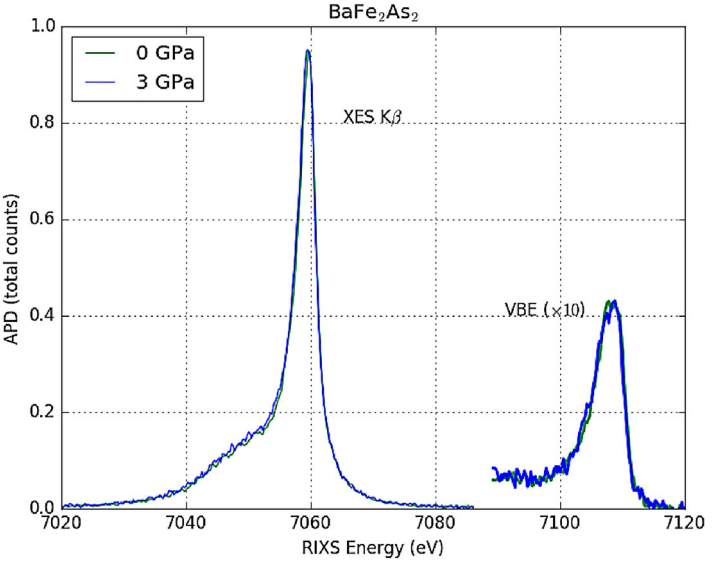

Figure 7. Kβ and valence band emission spectra in the 122 Fe-based superconductors under pressure.

family *cf.* Figure 7. In spite of its weak intensity, the VBE interestingly combines information about the chemical and magnetic environment.[31] Although resolution is lacking, the VBE in the 112 confirm the surprising stability of the Fe 3d electronic structure under pressure.

4. Conclusions and perspectives

In conclusion, hard-X-ray RIXS is a powerful method of investigation of the electronic and magnetic properties of materials under extreme conditions. RIXS can help investigate the empty density states, local spin states, chemical environment or low energy excitations with the advantage of bulk sensitivity and high resolution. RIXS was evoked here from the vantage point of oxides and Fe superconductors but has been applied to other correlated materials, including heavy fermions materials or more recently iridates. The advent of far more powerful X-ray sources in a near future [32] (the so-called diffraction limited storage rings) will open up new avenues for RIXS under pressure. With a gain of 1–2 orders of magnitude in brightness, high pressure RIXS up to the TPa regime will be possible using miniaturized anvils.[33]

On the other hand, a new generation of RIXS instrument combining a large array of analyzer crystals and 2D detectors will offer higher resolution while maintaining a high throughput, opening up new possibilities for investigating correlated materials at extreme conditions.

Disclosure statement

No potential conflict of interest was reported by the authors.

ORCiD

J.-P. Rueff http://orcid.org/0000-0003-3594-918X

References

[1] Mattila A, Rueff J-P, Badro J, Vankó G, Shukla A. Metal-ligand interplay in strongly-correlated oxides:a parametrized phase diagram for pressure induced spin transitions. Phys Rev Lett. 2007;98:196404.
[2] Ament LJP, Veenendaalvan M, Devereaux TP, Hill JP, Brinkvan den J. Resonant inelastic X-ray scattering studies of elementary excitations. Rev Mod Phys. 2010;83:705–767.
[3] Rueff J-P, Shukla A. Inelastic X-ray scattering by electronic excitations under high pressure. Rev Mod Phys. 2010;82:847–896.
[4] Caliebe WA, Kao CC, Hastings JB, et al. 1*s*2*p* resonant inelastic x-ray scattering in α-Fe_2O_3. Phys Rev B. 1998;58:13452–13458.
[5] Groot de FMF, Glatzel P, Bergmann U, et al. 1s2p resonant inelastic X-Ray scattering of iron ixides. J Phys Chem B. 2005;109:20751–20762.
[6] Sikora M, Juhin A, Weng T-C, et al. Strong K-Edge magnetic circular dichroism observed in Photon-in–Photon-out spectroscopy. Phys Rev Lett. 2010;105:037202.
[7] Wilke M. Spectroscopy of low Z elements at extreme conditions: in situ studies of Earth materials at pressure and temperature via X-ray Raman scattering. J High Pressure Res. 2016: Article no. 1198903. doi: 10.1080/08957959.2016.1198903
[8] Hiraoka N. EXAFS study under high-pressure by x-ray Raman scattering. J High Pressure Res. 2016: Article no. 1206090. doi: 10.1080/08957959.2016.1206090

[9] Rueff J-P, Ablett JM, Céolin D, et al. The GALAXIES beamline at SOLEIL synchrotron: inelastic X-ray scattering and photoelectron spectroscopy in the hard X-ray range. J Synchrotron Rad. 2015;22:175–179.
[10] Yamaoka H. Pressure dependence of the electronic structure of 4f and 3d electron systems studied by x-ray emission spectroscopy. J High Pressure Res. 2016: Article no. 1203914 doi: 10.1080/08957959.2016.1203914
[11] Boerde J, Verwey E. Semi-conductors with partially and with completely filled 3d-lattice bands. Proc Phys Soc. 1937;49:59–71.
[12] Mott N. Discussion of the paper by de Boer and Verwey. Proc Phys Soc. 1937;49:72–73.
[13] Hubbard J. Electron correlations in narrow energy bands. Proc R Soc Lond. 1963;276:238–257.
[14] Held K. Electronic structure calculations using dynamical mean field theory. Adv Phys. 2007;56:829–926.
[15] McWhan DB, Menth A, Remeika JP, Brinkman WF, Rice TM. Metal-insulator transitions in pure and doped V_2O_3. Phys Rev B. 1973;7:1920–1932.
[16] Park JH, Tjeng LH, Tanaka A, et al. Spin and orbital occupation and phase transitions in V_2O_3. Phys Rev B. 2000;61:11506–11509.
[17] Rodolakis F, Hansmann P, Rueff JP, et al. Inequivalent routes across the Mott transition in V_2O_3 explored by X-Ray absorption. Phys Rev Lett. 2010;104:047401.
[18] Rodolakis F, Rueff J-P, Sikora M, et al. Evolution of the electronic structure of a Mott system across its phase diagram: X-ray absorption spectroscopy study of $(V_{1-x}Cr_x)_2O_3$. Phys Rev B. 2011;84:245113.
[19] Lupi S, Baldassarre L, Mansart B, et al. A microscopic view on the Mott transition in chromium-doped V_2O_3. Nat Comm. 2010;1:105.
[20] Morin FJ. Oxides which show a metal-to-insulator transition at the neel temperature. Phys Rev Lett. 1959;3:34–36.
[21] Marezio M, McWhan DB, Remeika JP, Dernier PD. Structural aspects of the metal-insulator transitions in Cr-Doped VO_2. Phys Rev B. 1972;5:2541–2551.
[22] Arcangeletti E, Baldassarre L, Di Castro D, et al. Evidence of a pressure-induced metallization process in monoclinic VO_2. Phys Rev Lett. 2007;98:196406.
[23] Mitrano M, Maroni B, Marini C, et al. Anisotropic compression in the high-pressure regime of pure and chromium-doped vanadium dioxide. Phys Rev B. 2012;85:184108.
[24] Balédent V, Cerqueira TTF, Sarmiento-Pérez R, et al. Novel monoclinic M3 phase of VO2 from the combination of high-pressure Raman scattering and ab initio structural search. Phys Rev Lett. 2016, in press.
[25] Bai L, Li Q, Corr SA, et al. Pressure-induced phase transitions and metallization in VO_2. Phys Rev B. 2015;91:104110.
[26] Wu JJ, Lin JF, Wang XC, et al. Pressure-decoupled magnetic and structural transitions of the parent compound of iron-based 122 superconductors BaFe2As2. Proc Natl Acad Sci. 2013;110:17263–17266.
[27] Balédent V, Rullier-Albenque F, Colson D, Monaco G, Rueff JP. Stability of the Fe electronic structure through temperature-, doping-, and pressure-induced transitions in the $BaFe_2As_2$ superconductors. Phys Rev B. 2012;86:235123.
[28] Balédent V, Rullier-Albenque F, Colson D, Ablett J, Rueff JP. Electronic properties of $BaFe_2As_2$ upon doping and pressure: the prominent role of the As *p* orbitals. Phys Rev Lett. 2015;114:177001.
[29] Wadati H, Elfimov I, Sawatzky GA. Where are the extra d electrons in transition-metal-substituted iron pnictides? Phys Rev Lett. 2010;105:157004.
[30] Groot de FMF. High resolution x-ray emission and x-ray absorption spectroscopy. Chem Rev. 2001;101:1779–1808.
[31] Pollock CJ, DeBeer S. Insights into the geometric and electronic structure of transition metal centers from valence-to-core X-ray emission spectroscopy. Acc Chem Res. 2015;48:2967–2975.
[32] Castelvecchi D. Next-generation X-ray source fires up. Nature. 2015;525:15–16.
[33] Dubrovinsky L, Dubrovinskaia N, Bykova E, et al. The most incompressible metal osmium at static pressures above 750 gigapascals. Nature. 2015;525:226–229.